Chinese Chemical Letters 37 (2026) 112521

Contents lists available at ScienceDirect

Chinese Chemical Letters

journal homepage: www.elsevier.com/locate/cclet

Panchromatic solar absorption enables multi-photon CO_2 carboxylation: Mechanistic insights in consecutive photoinduced electron transfer

Limei Tian[a], Rong Liu[a], Zijian Zhao[a], Pengju Li[a], Weijian Yang[a], Fushuang Niu[c], Ke Hu[a,b,*]

[a] Department of Chemistry, Fudan University, Shanghai 200433, China
[b] School of Chemical Science and Engineering, Tongji University, Shanghai 200092, China
[c] School of Materials Science and Engineering, Linyi University, Linyi 276000, China

ARTICLE INFO

Article history:
Received 23 July 2025
Revised 10 February 2026
Accepted 11 February 2026
Available online 11 February 2026

Keywords:
Solar energy conversion
Dicarboxylation
Panchromatic absorption
CO_2 utilization
Consecutive photoinduced electron transfer

ABSTRACT

Inspired by natural photosynthesis, visible-light-driven carboxylation of carbon dioxide for the synthesis of value-added chemicals has attracted considerable attention. However, the current limitation in carboxylation lies in the narrow absorption range of the photocatalysts used. These photocatalysts are predominantly activated by blue light, limiting the utilization of most of the solar light. Herein, we employed the organic dye *N,N*-bis(2,6-diisopropylphenyl)perylene-3,4,9,10-bis(dicarboximide) (PDI), along with its single-electron-reduced state $PDI^{\bullet-}$ through consecutive photoinduced electron transfer (ConPET), effectively absorbs panchromatic solar spectrum for photocatalytic dicarboxylation. Mechanistic investigations using femtosecond time-resolved transient absorption (fs-TA) spectroscopy unequivocally identified the excited state of the singly reduced species, $PDI^{\bullet-*}$, rather than the doubly reduced form, as the key intermediate responsible for the reductive activation of alkenes. Furthermore, efficient solar-driven carboxylation of CO_2 was successfully demonstrated under natural sunlight irradiation, underscoring the practical potential of this photocatalytic system.

© 2026 Published by Elsevier B.V. on behalf of Chinese Chemical Society and Institute of Materia Medica, Chinese Academy of Medical Sciences.

Carboxylic acid derivatives play a pivotal role in the synthesis of pharmaceuticals [1,2], agrochemicals and value-added chemicals [3,4] such as dicarboxylic acids [5], amino acids [6], and heterocyclic compounds [7]. Carbon dioxide (CO_2) is a green and sustainable one-carbon (C_1) building block that is readily obtainable, non-flammable, non-toxic and inherently renewable [8–10]. Using CO_2 as a carboxylating agent for carboxylation of organic compounds is a vital transformation in the field of CO_2 utilization [11–13]. Unfortunately, the high kinetic and thermodynamic stability of CO_2 and the low reactivity of alkenes make it very difficult to directly convert CO_2 to carboxyl products.

By using sunlight to drive solar-to-chemical transformations, artificial photosynthesis mimics its natural counterpart and has attracted continued attention from chemists since 1912 [14]. The visible-light-driven photoredox catalysis provides an alternative pathway to realize carboxylation with CO_2 than the metal-catalyzed [15,16], offering significant advantages including mild reaction conditions, high efficiency, and facile operation [17–22]. Consequently, visible-light-induced or visible-light/transition metal dual-catalyzed regioselective carboxylation, silacarboxylation, phosphonocarboxylation, dicarboxylation as well as thiocarboxylation of alkenes have been developed with CO_2 and various radical precursors [16–18,23–37]. However, the photocatalysts used in these prior reports, including organic photocatalysts [38,39] and Iridium based metal complexes photocatalysts [40], generally exhibited an absorption range <500 nm. The limited absorption range significantly restricts the utilization of the solar spectrum. High energy photon in blue region remains one of the predominant factors for driving photocatalytic CO_2 carboxylation reactions (Fig. 1). The reliance on blue light excitation lies on the compromise between single photon energy and the excited state potency. Long wavelength (>500 nm) photon absorption generally means weaker excited state redox ability that would be sufficient to initiate the energy-demanding carboxylation of alkenes. Hence, the efficient utilization of photon energy in full solar spectrum to drive CO_2 carboxylation reactions still remains a great challenge.

Recently, consecutive photo-induced electron transfer (ConPET) approach emerged to overcome the limitation by harnessing the energies of two photons within a single catalytic cycle [41–46]. Although several studies have reported carboxylation reactions en-

* Corresponding author.
E-mail address: khu@tongji.edu.cn (K. Hu).

https://doi.org/10.1016/j.cclet.2026.112521
1001-8417/© 2026 Published by Elsevier B.V. on behalf of Chinese Chemical Society and Institute of Materia Medica, Chinese Academy of Medical Sciences.

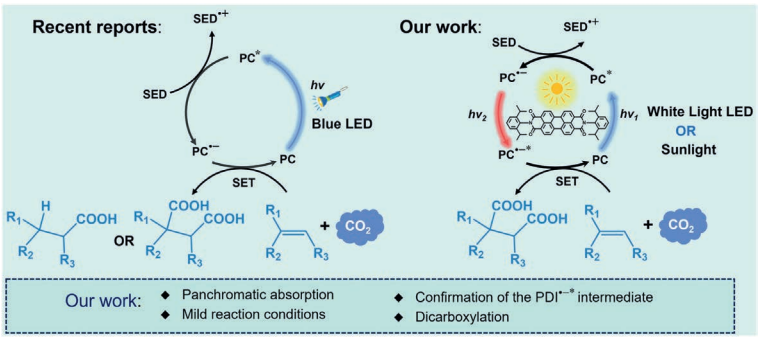


Fig. 1. Photocatalytic reductive carboxylations with CO_2. PC = photocatalyst, SED = sacrificial electron donor.

abled by ConPET process, mechanistic validation has primarily relied on nuclear magnetic resonance titration and density functional theory calculations [47–50]. Therefore, this study is dedicated to elucidating reaction intermediates in photoreaction processes using time-resolved transient absorption (TA) spectroscopy. Note that this study specifically targets the mechanism of ConPET through TA and reaction order.

Herein, we present the ConPET-mediated carboxylation of alkenes with CO_2, employing *N,N*-bis(2,6-diisopropylphenyl)-perylene-3,4,9,10-bis(dicarboximide) (PDI) as the key photocatalyst (Fig. 1). We specifically evaluated the Solar-to-chemical conversion efficiency of PDI compared with other commonly used photocatalysts. Furthermore, to elucidate the ConPET process, our study presented key experimental evidence. Specifically, by employing femtosecond time-resolved transient absorption (fs-TA) spectroscopy, we have achieved direct observation of the critical excited-state species and systematically monitored its bimolecular quenching kinetics. To further assess the practicality of our approach, a model carboxylation reaction under sunlight was carried out.

We started the selection of photocatalysts through the following criteria: (i) Developing panchromatic solar absorption photocatalysts and (ii) establishing mechanistic frameworks *via* combined fs-TA to resolve key intermediates. Despite the demonstrated advantages of PDI in photoredox catalysis, its application in CO_2 carboxylation reactions remains unexplored. Accordingly, we demonstrated the photocatalytic dicarboxylation of 1,1-diphenylethylene (**1a**) with CO_2 under white-light irradiation, affording 2,2-diphenylsuccinic acid (**2a**) with high efficiency. After a systematic investigation (Tables S1-S5 in Supporting information), the desired product **2a** was obtained in a 72.2 % isolated yield when using PDI as the photocatalyst, *N,N*-diisopropylethylamine (DIPEA) as the electron donor, *N,N*- dimethylformamide (DMF) as the solvent and Cs_2CO_3 as the base. Under the optimized conditions, the scope of activated alkenes was evaluated. The reaction demonstrated good compatibility with 1,1-diarylethylene derivatives, monoaryl-substituted alkenes and thiophene-based heterocyclic substrates. The results were shown in Fig. S2 (Supporting information). Detailed characterization of reactive intermediates involved in the reaction pathway is provided in Supporting information [51–56].

4CzIPN and Ir(ppy)$_3$, where ppy is 2-phenylpyridine, are two of the most commonly used photocatalysts for carboxylation reactions. Therefore, we compared PDI with the two photocatalysts. The UV–vis absorption spectra of the three photocatalysts are shown in Fig. 2. All three photocatalysts exhibited absorption in blue light region. However, PDI has a larger molar extinction coefficient and a broader absorption range. Subsequently, these three photocatalysts were employed to catalyze the model reaction under the previously optimized conditions. The yield of PDI was 3-fold higher than that of the other two photocatalysts. To facilitate

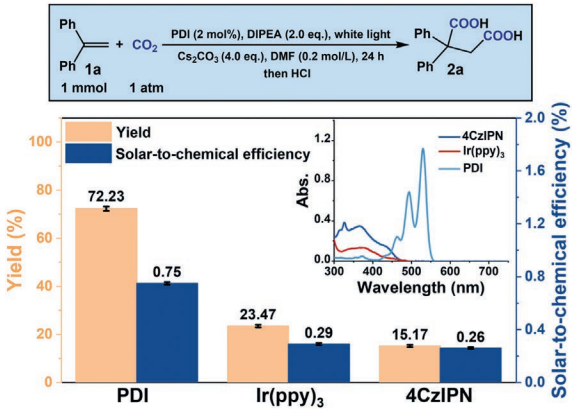


Fig. 2. Yield (left axis) and Solar-to-chemical efficiency (right axis) of dicarboxylation reaction of model substrate **1a** using different PCs. Error bars (black lines) depict the standard deviation from three independent experiments ($n = 3$). Inset: The UV–vis absorption spectra of different photocatalysts at the same concentrations (20 μmol/L), solvents (DMF) and other test conditions.

the comparison of photocatalytic performance among diverse photocatalysts, we introduced the apparent quantum efficiency (AQE), a metric defined as the ratio of the number of photons required for actual product generation to the total of incident photons [57,58]. Analogous to the Solar-to-hydrogen (STH) efficiency metric, AQE quantitatively represents the Solar-to-chemical energy conversion efficiency in our model reaction system [59,60]. For clarity and consistency, we hereafter refer to this quantity as the Solar-to-chemical efficiency and it is calculated using the following equation:

$$\text{Solar-to-chemical efficiency} = \frac{N_e}{N_p} \times 100\% = \text{AQE} = \frac{2 \times M \times N_A \times h \times c}{I_0 \times \lambda} \times 100\% \quad (1)$$

$$I_0 = S \times P \times t \quad (2)$$

Where N_p is the total incident photons, N_e is the total reactive electrons, M is the molar amount of **2a**, N_A is Avogadro constant, h is the Planck constant, c is the speed of light, I_0 is the total intensity of light emitted by the light source throughout the reaction, S is the irradiation area, P is the intensity of irradiation light, t is the photoreaction time, λ is the wavelength of the light. For detailed methodologies regarding the calculation of Solar-to-chemical efficiency, please refer to the experimental section in Supporting information. The comparison demonstrated that the Solar-to-chemical efficiency of PDI was two to three times higher than 4CzIPN and Ir(ppy)$_3$, in Fig. 2. These findings indicated that PDI showed the best photocatalytic performance and efficient utilization of white light in these catalysts.

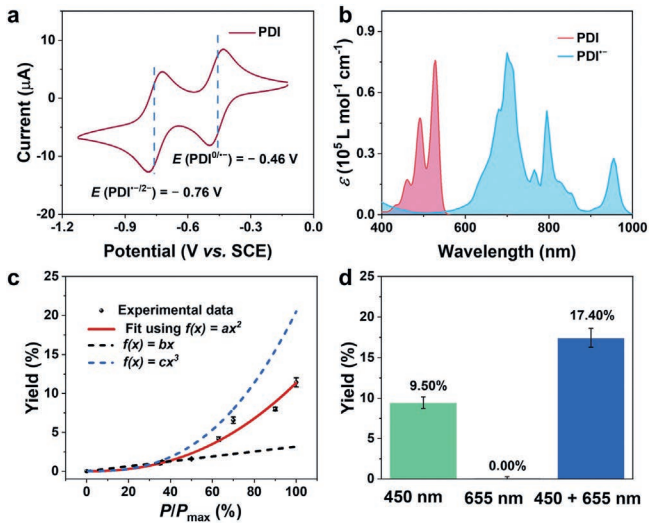


Fig. 3. (a) Cyclic voltammograms of PDI measured in 0.1 mol/L TBAP/MeCN. (b) Molar extinction coefficients of PDI and $PDI^{\bullet-}$ in DMF, and $PDI^{\bullet-}$ was chemically reduced by adding TDAE to the solution under N_2 atmosphere. (c) Dependence of initial yield of **2a** formation with different photon power densities under white light LED. The experimental data (solid black circles) are depicted with error bars indicating the standard deviation ($n = 3$ independent experiments). The experimental data were used to fit and found that the photon flux and yield were quadratic (red line). Black and blue dashed lines are hypothetical linear and cubic fits based on two low photon flux data. (d) Yield of **2a** after 24 h of different wavelengths of irradiation. The reported yields are averages from three parallel experiments.

As is well known, PDI, monoanion ($PDI^{\bullet-}$) and dianion (PDI^{2-}) have distinct light-absorbing properties, each exhibiting different optical characteristics and reduction capabilities [41]. Comparative studies, including intensity-dependence on yield, investigations at different irradiation wavelengths, and intermediate detection experiments, were carried out to determine which redox form of PDI excited state was responsible for one-electron reduction of alkene. Cyclic voltammograms of PDI displayed two distinct waves (Fig. 3a), corresponding to the consecutive reduction of the PDI cores to the $PDI^{\bullet-}$ and PDI^{2-}. PDI exhibited strong absorption in the visible light region, enabling it to absorb significant amounts of blue light (Fig. 3b, pink). Under photoreduction (Fig. S8 in Supporting information) conditions employing DIPEA as a sacrificial reductant, PDI was only accessible as its one-electron reduced radical anion state [41]. Similarly, treatment of PDI with tetrakis(dimethylamino)ethylene (TDAE) as a chemical reductant afforded exclusively the $PDI^{\bullet-}$ (Fig. 3b, blue). The absorption range of PDI and $PDI^{\bullet-}$ were complementary, enabling them to absorb most visible and some infrared light. Each of these species absorbed photons at different wavelengths, thereby customizing photon absorption for each redox event. This facilitated the productive utilization of light with wavelengths extending up to 1000 nm, and represented a distinct method for visible light utilization. Therefore, PDI could irradiate by white light, enhancing solar energy utilization for efficient photocatalysis.

Related consecutive photon mechanisms have previously been reported in the context of photocatalysis [61,62]. Mechanistic insight into photoredox reactions that rely on multi-photon excitation can also be obtained by analyzing the dependence of the product yield on the excitation power (P). In the initial phase of a biphotonic reaction, it is often expected that the product yield will show a quadratic dependence on P [40,63]. We studied the variation of the initial rate of **2a** formation with photon flux density, based on the relationship between the reaction yield and time (Fig. S9 in Supporting information). The reaction was carried out for 2 h under optimized reaction conditions, and the photon flux was varied by a combination of neutral density filters after the white light (Fig. 3c and Fig. S10 in Supporting information). The experimental data were used to fit and found that the photon flux and yield were quadratic (red line) which corroborated with the two-photon nature of the catalytic reaction. Linear (black line) and cubic (blue line) fitting to the first few data points clearly did not follow the data points across the whole power density range, indicating the absorption of two photons during the reaction. To verify the consecutive photon mechanism, different irradiation wavelengths experiment was conducted. When PDI was exposed to a 450 nm laser light source, **2a** formed with a yield of 9.5 % after 24 h. As expected, no **2a** was formed when irradiated with a 655 nm laser light source, as PDI exhibited minimal absorption at 655 nm. Remarkably, concurrent irradiation at 450 and 655 nm resulted in an enhanced yield of 17.4 % for product **2a** (Fig. 3d). Consequently, it was concluded that the second photon absorption by $PDI^{\bullet-}$ was crucial for achieving a high yield. The utilization of a white light source significantly improved which was attributed to the enhanced long wavelength absorption by PDI and $PDI^{\bullet-}$.

Subsequently, the photoreaction process was systematically investigated. Only PDI absorbed white light, while diphenylethylene compounds had hardly any absorption in the visible region (Fig. S11 in Supporting information). Consequently, white light irradiation predominantly generated the excited state PDI (PDI^*). Furthermore, Stern-Volmer quenching showed the PDI^* was quenched by DIPEA ($E_{p/2} = 0.91$ V *vs.* SCE, Fig. S12 in Supporting information), rather than by 1,1-diphenylethylene (Figs. S14 and S15 in Supporting information). This observation indicated that an electron transfer occurs from DIPEA to the photoexcited PDI, generating $PDI^{\bullet-}$, which thereby enabled its subsequent photoexcitation. In previous studies, it was challenging to ascertain whether the active substance of the reducing substrate was $PDI^{\bullet-*}$ or the PDI^{2-*} [64]. As illustrated in Fig. S13 (Supporting information), the reduction potential of 1,1-diphenylethylene is determined to be −1.79 V *vs.* SCE. According to previous reports, both $PDI^{\bullet-*}$ and PDI^{2-*} were favorable for alkene reduction due to their suitable potential ($E(PDI^{0/\bullet-*}) = -1.9$ V *vs.* SCE [65] and $E(PDI^{\bullet-/2-*}) = -2.6$ V *vs.* SCE [66]). However, when monitoring the spectral changes of the reaction system under white light, only $PDI^{\bullet-}$ was generated, with negligible PDI^{2-} in Fig. S17 (Supporting information). What is more, there was negligible absorption signal of PDI^{2-} observed in nanosecond transient absorption spectroscopy upon the excitation of $PDI^{\bullet-}$ and DIPEA, ruling out the possibility of electron transfer between $PDI^{\bullet-*}$ and DIPEA in Fig. S18 (Supporting information).

To unambiguously identify active intermediates in photoredox processes and elucidate the kinetic behavior of reactive species, we systematically investigated $PDI^{\bullet-}$ using femtosecond transient absorption spectroscopy [64]. Under inert conditions in a nitrogen-purged glovebox, stoichiometric reduction of the PDI was achieved using TDAE as the reducing agent, yielding $PDI^{\bullet-}$ with quantitative conversion (Fig. S19 in Supporting information). Global analysis of the transient absorption data (Fig. 4a) revealed characteristic excited-state absorption bands at 460 nm and 610 nm following 680 nm femtosecond laser excitation. Concurrently, ground-state bleaching signals in the 700–850 nm region corresponded to depletion of the electronic ground state population. Single-exponential fitting of the kinetic decay at the diagnostic 600 nm wavelength (Fig. S21 in Supporting information) yielded an excited state lifetime of 156 ps for $PDI^{\bullet-}$, consistent with literature values [64]. Quenching kinetics were probed by monitoring the excited-state absorption at 600 nm. Introduction of **1a** into the $PDI^{\bullet-}$ system induced a shortening of the lifetime of $PDI^{\bullet-*}$, demonstrating effective dynamic quenching by **1a**. Fig. 4b displayed the excited-state decay profiles across a concentration gradient of **1a** (0–0.45 mol/L). Systematic lifetime attenuation of $PDI^{\bullet-*}$ was observed with increasing quencher concentration, consistent with

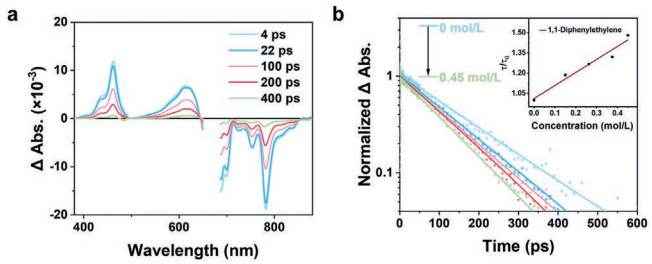


Fig. 4. (a) Femtosecond transient absorption spectra of $PDI^{\bullet-}$ in N_2 purged DMF solution, showing the $PDI^{\bullet-*}$ transient absorption features. (b) Normalized transient absorption kinetic traces monitored at 600 nm of 50 μmol/L $PDI^{\bullet-}$ with various concentrations of **1a**. Symbols represent experimental data and solid lines correspond to single-exponential fits. Inset: Stern-Volmer plot based on the experiment upon titration of **1a**.

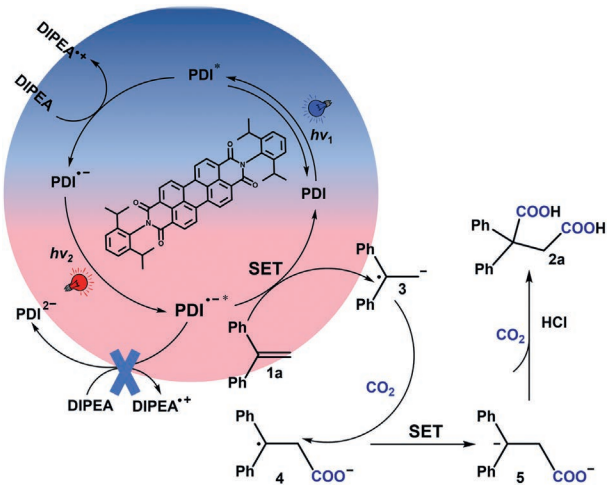


Fig. 5. Proposed mechanism for photocatalytic decarboxylation of 1,1-diphenylethylene and CO_2.

concentration-dependent quenching behavior. Linear regression of concentration-dependent data through Stern-Volmer analysis (Fig. S22 in Supporting information) afforded a second-order rate constant $k_q = 6.2 \times 10^9$ L mol^{-1} s^{-1}. TA kinetics provide definitive spectroscopic evidence for direct electron transfer from $PDI^{\bullet-*}$ to the alkene substrate. This spectroscopic signature unambiguously establishes $PDI^{\bullet-*}$, not the PDI^{2-*}, as the active reductant in the photocatalytic cycle, delivering critical experimental validation for the proposed ConPET pathway.

Based on the findings outlined above and in conjunction with previous reports, a plausible mechanism is proposed and shown in Fig. 5. The proposed mechanism involves the consecutive absorption of two photons: PDI initially absorbs the first photon, leading to the formation of PDI*. PDI* undergoes reductive quenching with DIPEA, resulting in the radical anion intermediate $PDI^{\bullet-}$. The second photon is subsequently absorbed by $PDI^{\bullet-}$ to produce $PDI^{\bullet-*}$. $PDI^{\bullet-*}$ then functions as a reducing agent, converting **1a** into its benzylic radical anion through diffusional encounters, which subsequently reacts with CO_2 to generate the intermediate **4**. Assuming that intermediate **4** further undergoes a second single electron transfer with an electron donor to generate benzylic anion **5**, which then reacts with a second CO_2 and undergoes protonation to give the desired product **2a**.

To validate the practical value of this strategy and exploit the catalyst's absorption performance, experiments were carried out using natural sunlight instead of a plug-in artificial light source [67–70]. The combined absorption spectra of PDI and $PDI^{\bullet-}$ cover most part of the solar spectrum in the visible region (Fig. 6a). As

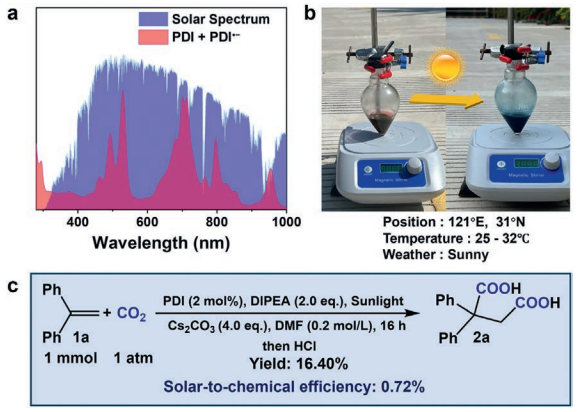


Fig. 6. (a) Overlay of the UV–vis-NIR absorption spectra of PDI + $PDI^{\bullet-}$ (pink) and AM 1.5G solar spectrum (purple). (b) The reaction color change of the reaction solution under natural sunlight (light intensity: 91.2 mW/cm^2). (c) Yield of product **2a** and Solar-to-chemical efficiency of PDI under natural sunlight.

shown in Fig. 6b, the color of the reaction solution changed from dark red to blue, indicating the generation of $PDI^{\bullet-}$ under sunlight. The reaction yield reached 16.4 % when PDI was used as the photocatalyst when the reaction was carried out under sunlight for two consecutive days (with 16 h of sunlight exposure, in Fig. 6c). In contrast, under identical conditions, the commonly used photocatalyst 4CzIPN afforded a yield of only 1.2 % (Figs. S23 and S24 in Supporting information). The yield with PDI as a photocatalyst was approximately 15 times than 4CzIPN.

In summary, we demonstrate a consecutive photoexcitation strategy using a broad-spectrum visible-light-responsive photocatalyst for efficient alkene carboxylation with CO_2 to dicarboxylic acids. Crucially, PDI exhibits 2–3-fold enhanced white-light utilization efficiency over conventional systems, establishing a new paradigm for solar driven synthesis. Mechanistic studies reveal a nonlinear multiphoton absorption process wherein sequential 400–600 nm and 600–1000 nm photons are harvested by both PDI and $PDI^{\bullet-}$. This panchromatic solar multiphoton absorption enables the generation of high-energy excited states while utilizing the major energy portion of solar spectrum. Crucially, to the best of our knowledge, it was first evidenced by fs-TA that $PDI^{\bullet-*}$ rather than PDI^{2-*} was the key electron donor for reductive activation of alkenes. The mechanistic insights into the $PDI^{\bullet-*}$-mediated ConPET mechanism, combined with the tunability of the PDI molecular core [71,72], provide a general framework for the rational design of efficient photocatalysts tailored for diverse CO_2 carboxylation systems. Remarkably, sunlight-driven reactions achieve high yield, providing a practical blueprint for efficient CO_2 utilization *via* natural sunlight harvesting.

CRediT authorship contribution statement

Limei Tian: Writing – original draft, Investigation, Formal analysis, Data curation. **Rong Liu:** Investigation. **Zijian Zhao:** Investigation, Funding acquisition. **Pengju Li:** Formal analysis, Data curation. **Weijian Yang:** Formal analysis. **Fushuang Niu:** Formal analysis. **Ke Hu:** Writing – review & editing, Visualization, Validation, Supervision, Resources, Project administration, Methodology, Funding acquisition, Conceptualization.

Declaration of competing interest

The authors declare that they have no known competing financial interests or personal relationships that could have appeared to influence the work reported in this paper.

Acknowledgments

This work is sponsored by the National Key R&D Program of China (No. 2023YFE0124100), the National Natural Science Foundation of China (No. 22173022), the Fundamental Research Funds for the Central Universities, and the China Postdoctoral Science Foundation (Nos. 2025T180305, 2024M760508, GZB20240159).

Supplementary materials

Supplementary material associated with this article can be found, in the online version, at doi:10.1016/j.cclet.2026.112521.

References

[1] J. Bai, M. Li, C. Zhou, et al., Org. Lett. 23 (2021) 9654–9658.
[2] Z. Fan, Z. Zhang, C. Xi, ChemSusChem 13 (2020) 6201–6218.
[3] H. Hahm, D. Baek, D. Kim, et al., Org. Lett. 23 (2021) 3879–3884.
[4] C. Zhou, M. Li, J. Yu, et al., Chin. J. Org. Chem. 40 (2020) 2221–2231.
[5] W. Zhang, L.L. Liao, L. Li, et al., Angew. Chem. Int. Ed. 62 (2023) e202301892.
[6] T. Ju, Q. Fu, J.H. Ye, et al., Angew. Chem. Int. Ed. 57 (2018) 13897–13901.
[7] Y.M. Tian, H. Wang, Ritu, et al., Chem. Sci. 13 (2022) 241–246.
[8] J.H. Ye, T. Ju, H. Huang, et al., Acc. Chem. Res. 54 (2021) 2518–2531.
[9] T. Sakakura, J.C. Choi, H. Yasuda, Chem. Rev. 107 (2007) 2365–2387.
[10] H. Luo, J. Ren, Y. Sun, et al., Chin. Chem. Lett. 34 (2023) 107782.
[11] Y. Kim, G.D. Park, M. Balamurugan, et al., Adv. Sci. 7 (2020) 1900137.
[12] N.W.J. Ang, J.C.A. Oliveira, L. Ackermann, Angew. Chem. Int. Ed. 59 (2020) 12842–12847.
[13] S. Pradhan, S. Roy, B. Sahoo, et al., Chem. Eur. J. 27 (2021) 2254–2269.
[14] G. Ciamician, Science 36 (1912) 385–394.
[15] M.D. Greenhalgh, S.P. Thomas, J. Am. Chem. Soc. 134 (2012) 11900–11903.
[16] J. Zhou, L. Hu, R. Wang, et al., Chin. Chem. Lett. 37 (2026) 111304.
[17] Y. Huang, J. Hou, L.W. Zhan, et al., ACS Catal. 11 (2021) 15004–15012.
[18] C.K. Ran, Y.N. Niu, L. Song, et al., ACS Catal. 12 (2022) 18–24.
[19] Z. Zhang, J.H. Ye, T. Ju, et al., ACS Catal. 10 (2020) 10871–10885.
[20] M. Schmalzbauer, T.D. Svejstrup, F. Fricke, et al., Chem 6 (2020) 2658–2672.
[21] L. Wang, F. Shi, C. Qi, et al., Chem. Sci. 12 (2021) 11821–11830.
[22] H. Wang, Y. Gao, C. Zhou, et al., J. Am. Chem. Soc. 142 (2020) 8122–8129.
[23] T. Ju, Y.Q. Zhou, K.G. Cao, et al., Nat. Catal. 4 (2021) 304–311.
[24] W.D. Li, Y. Wu, S.J. Li, et al., J. Am. Chem. Soc. 144 (2022) 8551–8559.
[25] Q.Y. Meng, T.E. Schirmer, A.L. Berger, et al., J. Am. Chem. Soc. 141 (2019) 11393–11397.
[26] L. Song, W. Wang, J.P. Yue, et al., Nat. Catal. 5 (2022) 832–838.
[27] T. Yuan, Z. Wu, S. Zhai, et al., Angew. Chem. Int. Ed. 62 (2023) e202304861.
[28] X.W. Chen, J.P. Yue, K. Wang, et al., Angew. Chem. Int. Ed. 60 (2021) 14068–14075.
[29] Z. Fan, S. Chen, S. Zou, et al., ACS Catal. 12 (2022) 2781–2787.
[30] B. Zhang, Y. Yi, Z.Q. Wu, et al., Green Chem. 22 (2020) 5961–5965.
[31] C.K. Ran, H.Z. Xiao, L.L. Liao, et al., Natl. Sci. Open 2 (2023) 20220024.
[32] B. Yu, Y. Liu, H.Z. Xiao, et al., Chem 10 (2024) 938–951.
[33] H.X. Jiang, Z.T. Liu, P. Xu, et al., Chin. Chem. Lett. 36 (2025) 111224.
[34] H.Z. Xiao, B. Yu, S.S. Yan, et al., Chin. J. Catal. 50 (2023) 222–228.
[35] L.L. Liao, Z.H. Wang, K.G. Cao, et al., J. Am. Chem. Soc. 144 (2022) 2062–2068.
[36] W. Wang, S.S. Yan, Y. Liu, et al., J. Am. Chem. Soc. 147 (2025) 23715–23723.
[37] P. Li, C. Bourgois, F. Glaser, et al., J. Am. Chem. Soc. 147 (2025) 12082–12091.
[38] L. Chen, Q. Qu, C.K. Ran, et al., Angew. Chem. Int. Ed. 62 (2023) e202217918.
[39] T.Y. Gao, X.Y. Mo, S.R. Zhang, et al., Chin. Chem. Lett. 35 (2024) 109364.
[40] A. Chatterjee, B. König, Angew. Chem. Int. Ed. 58 (2019) 14289–14294.
[41] I. Ghosh, T. Ghosh, J.I. Bardagi, et al., Science 346 (2014) 725–728.
[42] I.A. MacKenzie, L. Wang, N.P.R. Onuska, et al., Nature 580 (2020) 76–80.
[43] P. Li, A.M. Deetz, J. Hu, et al., J. Am. Chem. Soc. 144 (2022) 17604–17610.
[44] K. Targos, O.P. Williams, Z.K. Wickens, J. Am. Chem. Soc. 143 (2021) 4125–4132.
[45] W. Yang, P. Li, Y. Han, et al., Chem. Sci. 16 (2025) 20229–20238.
[46] Z. Zhao, J. Li, W. Yuan, et al., J. Am. Chem. Soc. 146 (2024) 1364–1373.
[47] Y. Liu, Z.H. Wang, G.H. Xue, et al., Chin. Chem. Lett. 35 (2024) 109138.
[48] K.G. Cao, T.Y. Gao, L.L. Liao, et al., Chin. J. Catal. 56 (2024) 74–80.
[49] Y. Liu, G.H. Xue, Z. He, et al., J. Am. Chem. Soc. 146 (2024) 28350–28359.
[50] X.Y. Wang, P. Xu, W.W. Liu, et al., Sci. China Chem. 67 (2024) 368–373.
[51] S. Zhao, S.S. Shen, L. Han, et al., Rare Met. 43 (2024) 4038–4055.
[52] X. Li, T. Han, Y. Zhou, et al., Sci. China Tech. Sci. 67 (2024) 1238–1252.
[53] X. Li, Q. Liu, F. Deng, et al., Appl. Catal. B: Environ. 314 (2022) 121502.
[54] L. Xiao, W. Ren, S. Shen, et al., Acta Phys. Chim. Sin. 40 (2024) 2308036.
[55] X. Li, Y. Wan, F. Deng, et al., Chin. Chem. Lett. 36 (2025) 111418.
[56] J. Ye, M. Ren, J. Qian, X. Li, et al., Chin. Chem. Lett. 36 (2025) 110857.
[57] X. Tao, Y. Zhao, S. Wang, et al., Chem. Soc. Rev. 51 (2022) 3561–3608.
[58] K. Maeda, M. Higashi, D. Lu, et al., J. Am. Chem. Soc. 132 (2010) 5858–5868.
[59] Y. Qi, Y. Zhao, Y. Gao, et al., Joule 2 (2018) 2393–2402.
[60] Y. Goto, T. Hisatomi, Q. Wang, et al., Joule 2 (2018) 509–520.
[61] J. Schneidewind, M.A. Argüello Cordero, H. Junge, et al., Energy Environ. Sci. 14 (2021) 4427–4436.
[62] H. Huang, X. Jing, J. Deng, et al., J. Am. Chem. Soc. 145 (2023) 2170–2182.
[63] F. Glaser, C. Kerzig, O.S. Wenger, Angew. Chem. Int. Ed. 59 (2020) 10266–10284.
[64] C.J. Zeman, S. Kim, F. Zhang, et al., J. Am. Chem. Soc. 142 (2020) 2204–2207.
[65] Z. Zhao, F. Niu, P. Li, et al., J. Am. Chem. Soc. 144 (2022) 7043–7047.
[66] H. Li, O.S. Wenger, Angew. Chem. Int. Ed. 61 (2022) e202110491.
[67] D. Cambié, J. Dobbelaar, P. Riente, et al., Angew. Chem. Int. Ed. 58 (2019) 14374–14378.
[68] T.J.B. Zähringer, M. Wienhold, R. Gilmour, et al., J. Am. Chem. Soc. 145 (2023) 21576–21586.
[69] L.L. Liao, G.M. Cao, Y.X. Jiang, et al., J. Am. Chem. Soc. 143 (2021) 2812–2821.
[70] X. Fan, X. Gong, M. Ma, et al., Nat. Commun. 9 (2018) 4936.
[71] Z.J. Zhang, X.J. Chen, H.J. Zhang, et al., Adv. Mater. 32 (2020) 1907746.
[72] S.F. Feng, Y.P. Zhang, H.H. Xu, et al., J. Alloy. Compd. 938 (2023) 168500.